HHS Public Access

Author manuscript

Ann N Y Acad Sci. Author manuscript; available in PMC 2021 November 01.

Published in final edited form as:

Ann N Y Acad Sci. 2020 November ; 1479(1): 75–93. doi:10.1111/nyas.14314.

NADPH Oxidase Inhibitor, Diapocynin, Counteracts Diisopropylfluorophosphate (DFP)-induced Long-term Neurotoxicity in the Rat Model

Marson Putra[1,2], **Meghan Gage**[1,2], **Shaunik Sharma**[2], **Cara Gardner**[2], **Grace Gasser**[3], **Vellareddy Anantharam**[3], **Thimmasettappa Thippeswamy**[1,2,#]

[1]Neuroscience Graduate Program, Iowa State University, Ames, IA 50011

[2]Department of Biomedical Sciences, College of Veterinary Medicine, Iowa State University, Ames, IA 50011.

[3]PK Biosciences Corporation, Ames, IA 50011

Abstract

Organophosphate (OP) nerve agents are a threat to both the military and civilians. OP exposure causes cholinergic crisis and *status epilepticus* (SE) due to irreversible inhibition of acetylcholinesterase that can be life-threatening if left untreated. OP survivors develop long-term morbidity such as cognitive impairment and motor dysfunction because of oxidative stress and progressive neuroinflammation and neurodegeneration (disease promoters). Current medical countermeasures (MCM) do not mitigate these pathologies. Therefore, our goal was to target disease promoters using diapocynin (DPO), an NADPH oxidase inhibitor, in addition to MCM, in the rat diisopropylfluorophosphate (DFP) model. The DFP-intoxicated rats were treated with diapocynin (300mg/kg, oral, six doses, 12h intervals) or vehicle 2h following behavioral SE termination with diazepam. The diapocynin treatment significantly rescued DFP-induced motor impairment, attenuated epileptiform spiking during the first 72h post-DFP in severely seizing rats despite no difference in epileptiform spike rate between the vehicle and diapocynin groups in mild SE rats. DPO significantly reduced DFP-induced reactive astrogliosis, neurodegeneration, $GP91^{phox}$, glutathiolated protein, serum nitrite, or pro-inflammatory cytokines and chemokines such as interleukins (IL) IL-1α, IL-6, IL-2, IL-17A, Leptin, IP-10 in the hippocampus. Collectively, these data support the neuroprotective role of diapocynin in an OP-induced neurotoxicity model.

Keywords

Neuroinflammation; Neurodegeneration; Oxidative stress; Chemical nerve agents; Organophosphate; Seizure

[#]Corresponding author: T. Thippeswamy, Epilepsy Research Laboratory, Department of Biomedical Science, 2036 College of Veterinary Medicine, Iowa State University, Ames, Iowa 50011. tswamy@iastate.edu Phone: 515-294-2571.

Conflict of interest

The authors declare no conflicts of interest.

Introduction

Exposure to organophosphate (OP) chemical nerve agents (OPNA) is a public health concern accounting for ~300,000 deaths annually worldwide[1,2]. OPNA were used in the Iran-Iraq war and Tokyo subway[3-6]. Recent civilian attacks with nerve agents in Syria, UK, and Malaysia suggest increased use of nerve agents as biochemical weapons in the future[5,7,8]. OPNA exposure causes irreversible inhibition of acetylcholinesterase and exacerbates cholinergic toxidrome leading to lethal parasympathomimetic symptoms (*status epilepticus* (SE) and respiratory and cardiac failure) as a result of overstimulation of muscarinic and nicotinic receptors[9,10]. While acute OP exposure can lead to death, neurological problems such as epilepsy, cognitive, and motor dysfunctions may occur in survivors[11,12]. Likewise, in experimental OPNA models, seizures and long-term behavioral deficits are common features of OP intoxication due to persistent gliosis, neurodegeneration, and oxidative stress[13-18]. The current medical countermeasures (MCM) for the OPNA symptoms include atropine and oximes to control respiratory and cardiac distress and benzodiazepines for seizures[10,19]. These MCM may suppress peripheral effects of the cholinergic crisis if administered in <10-15 minutes of OPNA exposure, which is unrealistic in a real-world scenario[19]. If delayed, MCMs fail to rescue systemic neuronal damage and associated brain dysfunction. Therefore, there is a need for the development of effective therapy to complement the existing MCM treatment regimen to counteract the long-term consequences of OPNA exposure survivors[11].

Growing evidence has supported the role of oxidative stress as a critical mediator in the pathology of OP toxicity and neuroinflammation observed in animal models of OP intoxication and human OP poisoning[20-24]. Both *in vivo* and *in vitro* studies have confirmed that direct OP exposure, as well as subsequent seizures in animal models, facilitates overproduction of reactive oxygen and nitrogen species (ROS/RNS) that can lead to brain injury[25-27]. One of the primary sources of ROS in neurodegenerative diseases is NADPH oxidase, an enzyme that is capable of reducing oxygen to form superoxide (O_2^-), which is detrimental to the cells. NOX2, one of the isoforms of NADPH oxidase, is reported to be highly expressed in neurons and glial cells in several brain regions[28,29]. Moreover, elevated mRNA and protein levels of NOX2 were observed in many neurological diseases, including epilepsy[28,30,31]. Therefore, we hypothesized that targeting NOX2 may be an important neuroprotective strategy to mitigate OPNA-induced neuronal damage and dysfunction. Some studies have demonstrated the neuroprotective effects of NOX2 inhibition or modulation, by reducing neuroinflammation, and improved behavioral function in chemoconvulsant-induced epilepsy models[32-34]. Recently, we demonstrated the role of nitro-oxidative stress in both kainate and diisopropylfluorophosphate (DFP)-induced epileptogenesis and cognitive and motor dysfunction[14,35]. These studies strongly support the role of oxidative stress in brain pathogenesis and the therapeutic potential of NOX2 inhibition.

In the present study, we used a plant-based antioxidant diapocynin (DPO), a dimeric derivative of apocynin, to test its neuroprotective effects in a rat model of DFP-induced long-term neurotoxicity. DFP is structurally similar to the nerve agent soman and therefore makes a useful surrogate for nerve agents that have been used in chemical warfare scenarios [36-38]. We report here that DPO significantly suppresses DFP-induced epileptiform spiking, rescues

motor learning deficits, attenuates reactive astrogliosis and neurodegeneration, reduces the level of GP91^{phox} (a membrane-associated NOX2 subunit) and glutathiolated protein (oxidative stress markers), serum nitrite and the pro-inflammatory cytokines and chemokines levels such as IL-1α, IL-6, IL-17A, leptin, and IP-10. Collectively, our results from the rat DFP model of neurotoxicity demonstrates a potential neuroprotective effect of NOX2 inhibition by DPO.

Materials and Methods

Animals

Adult male Sprague-Dawley rats (Charles River) weighing approximately 200g (7-8 weeks old) were used in these experiments. All rats were housed on a light/dark (12 hours on/12 hours off) cycle with ambient temperature 22±2°C and provided unlimited access to pelleted food and drinking water. The rats were acclimatized for 72 hours before experimentation. Animals were individually housed, and all animal care procedures pre and post DFP exposure were conducted in accordance with the guidelines of National Institutes of Health Guide for the Care and Use of Laboratory Animals and approved by the Iowa State University Institutional Animal Care and Use Committee (IACUC). The experiments conducted for this study complies with ARRIVE guidelines[39].

Experimental designs, DFP and DPO administration

As illustrated in experimental schematics (Fig. 1AB), both telemetered and non-telemetered rats were injected with 4 mg/kg of DFP (s.c.) in cold PBS (Sigma Aldrich, USA) and immediately co-treated with atropine sulfate (2 mg/kg, i.m.) and 2-pralidoxime (2-PAM, 25 mg/kg, i.m.) to reduce mortality caused by peripheral parasympathomimetic effects of DFP[40]. The development of SE was quantified for two hours. During this 2h period, the severity of behavioral SE was scored on a five-point staging scale as previously described[14]. Following 2h SE, diazepam was administered (Hospira Inc., 5 mg/kg, i.m) to control behavioral seizures. Additionally, to maintain hydration following SE, 1 mL of 5% dextrose saline was administered subcutaneously, followed by wet pelleted food until they could eat on their own (typically three days) and gained body weight. The degree of seizure burden during SE was quantified and the rats were equally distributed between treatment groups (vehicle and diapocynin (DPO)) to match the initial SE severity between groups (Fig. 1CD). DPO was constituted in 10% ethanol and administered orally (300 mg/kg every 12 hours for 72 hours) starting at 2h post-diazepam. Vehicle group rats received an equivalent volume of 10% ethanol. The rats implanted with telemetry were subjected to a continuous video-EEG recording for four weeks. Non-telemetry rats were used for various behavioral tests (Morris Water Maze, Rotarod, Horizontal Bar test) beginning ten days post-exposure (Fig. 1B) and euthanized at six weeks post-exposure.

DFP-induced behavioral seizures scoring

Seizures developed in <10 mins following DFP injection which were scored as described previously[14]: stage 1- excessive salivation, lacrimation, urination and defecation (SLUD), mastication, chewing; stage 2- tremors, wet-dog shakes, head nodding, neck jerks, kyphosis, and opisthotonus; stage 3- forelimb clonus, Straub tail, rearing and rigid extension of

forelimbs; stage 4- rearing, forelimb clonus and loss of righting reflex; and stage 5- abducted limbs clonus/repeated rearing and generalized seizures. Stage 1 and 2 seizures were non-convulsive seizures (NCS) while stage 3 to 5 were considered convulsive seizures (CS)[41]. Based on the duration of CS, the severity of SE was categorized into mild-moderate (<30 mins of CS) and severe (>30 mins of CS) SE. The vehicle and DPO groups had an equal number of animals from both mild-moderate and severe SE categories.

Electrode implantation, EEG recording, and epileptiform spikes analysis

In telemetered experiments, 17 animals were implanted with EEG radio transmitter device CTA-F40 (PhysioTel, Data Science International)[14,39] to monitor brain electrical activity following DFP intoxication and DPO treatment. Details of the surgery and post-operative care are included in Supplementary Materials. Baseline EEG was collected intermittently for ten days for normalization following DFP treatment and continued for further four weeks. The NeuroScore 3.2.0 software (DSI) was used for epileptiform spike detection and quantification. Movement artifacts and electrical spikes were manually removed from the EEG traces before the epileptiform spikes were quantified. The corresponding gamma, theta, and delta powers were used to confirm epileptiform spiking from artifacts in addition to spike duration on EEG traces.

The Morris Water Maze

The Morris water maze was used to test hippocampal-dependent spatial learning and memory[42] following DFP intoxication, as previously described[14]. The detailed experimental protocol is included in Supplementary Materials. The treatment groups were blinded to the experimenters. Baseline spatial learning and memory acquisition were collected and analyzed for all rats before DFP administration. Following DFP on day 10, another set of MWM test was conducted to evaluate the impact of DFP on spatial learning and memory. The amount of time spent in each quadrant during the 60 seconds swim was recorded, plotted, analyzed and compared between the groups and the quadrants.

Rotarod

All non-telemetered rats were tested for motor coordination, motor learning, and overall locomotor function using an accelerating rotarod apparatus AccuRotor 4 channel (Omnitech Electronics Inc.). Details about the apparatus have been previously described[14]. For each trial, the rats were trained on a 6-cm-diameter grooved rod starting at 5 rpm, accelerating to 60 rpm over 2 minutes. The rats were examined for latency to fall from the accelerating rod during each of three trials with 5 mins inter-trial intervals on training and testing days. Each trial completed when the rats fell off (distance of 15cm) the rod onto a cushioned lever. Baseline rotarod performance was acquired before DFP. Evaluation of motor learning and coordination on rotarod were conducted on day 18 post-DFP in all groups by measuring the amount of time spent on the rods (latency to fall) and compared with performances between training and test days.

Horizontal Bar Crossing Test

A horizontal bar test was performed to further test for static motor coordination, as previously described[14]. Briefly, an 80cm wooden bar with a diameter of 2.5 cm was placed spanning horizontally 58 cm above the ground between two metal rods. The rat crossed the bar to the secure box on the other end and time to reach the box was recorded for 90 seconds. Four trials were conducted during training day and only a single attempt on test day after 24h rest. Like other behavioral tests, baseline data were collected before DFP exposure. The time spent reaching the box were plotted and analyzed between groups, and training and test days.

Tissue collection and processing

For immunohistochemistry, the brains were collected after the animals euthanized at the end of each experiment with an overdose of pentobarbital (100 mg/kg, i.p.) as described previously[35]. Trans-Cardiac perfusion with PBS, followed by 4% paraformaldehyde in PBS was performed to fix the brain. The brains were post-fixed in 4% paraformaldehyde for overnight at 4°C, followed by immersion in 25% sucrose for 72h at 4°C. The hemispheres and cerebellum were separated prior to embedding with gelatin as previously described[14]. Each brain block was then mounted onto a cork disk and rapidly frozen in liquid nitrogen-cooled isopentane. Frozen brain blocks were sectioned coronally at 16 μm on a cryostat (Cryostar NX70, ThermoScientific). Brain sections were collected on gelatin-coated slides and stored at −80°C for further analysis. For biochemical studies, brain regions were dissected immediately after euthanasia and rapidly frozen in liquid nitrogen and stored at −80°C.

Immunohistochemistry, FJB, and cell quantification

The brain sections were subjected to heat-induced antigen retrieval by immersing the slides in pre-heated citrate buffer (10 mM citric acid, 0.05% Tween 20, pH 6) for 23 minutes at 90°C. Slides were mounted onto Shandon plastic cover plates (Thermoscientific) and processed for immunostaining. The details of immunostaining protocol, reagents, and antibodies (Table S1) used are included in Supplementary Materials.

To identify degenerating neurons, Fluoro-Jade B (FJB) staining was performed as previously described[14,35]. Following incubation with secondary antibodies for NeuN immunostaining, the sections were washed in PBS, immersed in distilled water (DW) for 1 min, and oxidized with 0.006% $KMnO_4$ in DW for 5 mins on a shaker. Sections were washed with DW for 3 mins with gentle agitation and then incubated for 10 mins with 0.0003% FJB stock in 0.1% acetic acid solution. Sections were then rinsed with DW, air-dried, cleared with xylene, and mounted with Acrytol (Surgipath, Leica Biosystems, IL).

All immunostained sections were visualized with an inverted fluorescence microscope Zeiss Axiovert 200 equipped with Hamamatsu digital camera (Model C-10600-10B). Representative images from various brain regions were captured and processed with HCImage 4.1.2 and analyzed using *ImageJ*. The immunopositive cells containing a visible DAPI marker were counted from a minimum of three sections per animal covering rostral to caudal regions of the hippocampus and piriform cortex, as previously described[14,35].

Investigators were blind to the samples assigned for cell quantification. Abercrombie correction was used in quantification to avoid over-counting bias while considering cell fractions as a whole-cell, as previously described[43]. The adjusted cell counts were then obtained from following equation: $P = A \cdot [M/(L + M)]$, P = corrected cell count, A = rough cell count, M = thickness of the section (μm), and L = mean width of 20 nuclei/section (μm).

Western Blotting

The frozen hippocampal tissues were homogenized in lysis buffer containing protease and phosphatase inhibitors (Thermo-Scientific, USA), as previously described[44]. The homogenates were centrifuged at 15000 x g for 1h at 4°C. The supernatants were collected and protein concentration was calculated using the Bradford method. In each lane, 20 μg of concentrated proteins were loaded and separated in 8-10% SDS-PAGE gels. The separated proteins were transferred onto a nitrocellulose membrane overnight and blocked. Membranes were incubated with primary antibodies diluted in fluorescent blocking buffer containing 0.05% Tween 20 overnight at 4°C. After washes with PBS, the membranes were incubated with infrared dye-tagged secondary antibodies, either 680 nm or 800 nm for 1h. Membranes were visualized using the Odyssey IR imaging system (LiCor, USA). *ImageJ* software was used to measure intensity of proteins bands. Antibodies details are available in Table S1. Representative results are shown in figure 7A and the full membrane blots can be found in the Supplementary Materials.

Nitrite assay

The Griess assay was performed as previously described[14]. Briefly, 50 μL of undiluted serum was plated onto a 96-well plate with a minimum of three replicates, and an equal volume of Griess reagent (Sigma-Aldrich) was added into the wells and incubated for 10 mins. The absorbance was measured at 540nm using a Synergy 2 multi-mode microplate reader (BioTek Instruments, USA). The readout was adjusted with sodium nitrite standard curve and values between samples were compared and analyzed.

Multiplex immunoassays

Hippocampal cytokines and chemokines levels were analyzed in duplicate using Millipore Multiplex Rat Cytokine/Chemokine Magnetic Bead Panel (Millipore) by Eve Technologies (Calgary, Alberta) as per the manufacturer's protocol, as previously described[14]. A panel of multiple markers was assayed in a protein concentration of 500 μg/ml which includes, Eotaxin, EGF, Fractalkine, IL-1α, IL-1β, IL-2, IL-4, IL-5, IL-6, IL-10, IL-12(p70), IL-17A, IL-18, IP-10, TNF-α, MCP-1, Leptin, LIX, RANTES, and VEGF. Each analyte was analyzed individually to identify statistical differences between groups.

Methodological rigor and data analyses

All animals were randomized and coded before used in the experiments. All investigators were blinded to the experimental groups until all the data were completely analyzed. Statistical analysis was performed using Prism 8 (GraphPad) and R-Studio version 1.1.463. The normality of data was evaluated using Shapiro-Wilk normality test, and outliers were detected with Robust Regression and Outlier Removal Test (ROUT). When comparing

multiple groups, data were analyzed with one-way ANOVA with Tukey's post hoc. Data with two factors were analyzed with repeated measures two-way ANOVA (general linear model) or mixed-effects model with Tukey's or Sidak's post hoc assuming equal variability of differences. As for two-group comparison, unpaired Student's t-test or Mann-Whitney were used. The summary of all statistical tests used in this study is available in Table S2 (Supplementary Materials). All data represent the mean and standard error mean (SEM) except for mixed-effects analysis in astrogliosis, microgliosis and neurodegeneration where the data were presented as group median with 95% of confidence interval. Differences indicated by $p<0.05$ were considered statistically significant.

Results

DPO suppresses DFP-induced epileptiform spikes during the treatment period

Subcutaneous DFP injection generated various stages of seizures in both telemetered and non-telemetered rats. The initial SE severity was quantified based on the duration of the stages of seizures occurred between the DFP exposure and diazepam treatment, typically two hours, as described in our recent publication[14]. The seizures were grouped as convulsive (stage 3 and above) and non-convulsive seizures (stage 1 and 2). There were no significant differences in the initial SE severity between the animals that received vehicle or DPO in both telemetry and non-telemetry groups (Fig. 1C, 1D). In telemetered group, three rats from the DFP+VEH and DFP+DPO groups developed severe SE and generated high numbers of epileptiform spikes (Fig. 2A, 2B). Therefore, we compared the effect of DPO treatment on epileptiform spike rate between these groups. DPO treated rats showed a significant decrease of epileptiform spikes in the first 72h post-DFP (Fig 2B). In the telemetered rats that had mild seizures during SE, occasional epileptiform spikes were observed which were correlated with the increase of theta (2-4 Hz) and delta (0-4 Hz) powers (Fig. 2C)[45]. Since there was no significant increase in epileptiform spikes during SE in both vehicle and DPO groups (Fig. 2D), we could not determine the real impact of DPO in the mild groups in contrast to the severe groups.

The effects of DPO on DFP-induced learning and memory impairments

DFP exposure causes hippocampal neurodegeneration as early as 24h post-exposure[46] suggesting that this may affect learning and memory in the long-term. To test this, Morris Water Maze (MWM) was performed with non-telemetered animals. Baseline data were collected from each animal and assigned to different treatment groups after DFP exposure. There were no differences in escape latencies between groups when the platform was placed in the water or the probe test when the platform was removed in pre-DFP tests. The rats had significantly less escape latencies on day 6 than on day 1 signifying the ability of rats to learn over training periods. As expected, there were significant differences in the time spent in the target quadrant (TQ) versus non-target quadrants (NTQs) in the probe trial (Fig. 3Ai, ii). When the animals were tested ten days after DFP exposure, both the vehicle and DPO groups exposed to DFP showed similar escape latencies and no significant differences were observed between day 1 and day 6, while the animals in the control group showed significantly shorter escape latencies (Fig. 3Bi) suggesting the impact of DFP, but not DPO, on spatial learning. There were no significant statistical differences in the overall learning

curves between groups. In the probe trial (at 16d post-DFP), the control rats spent a significant amount of time in the target quadrant than in the non-target quadrants implying memory retention. In contrast, neither the vehicle nor DPO treated DFP-exposed rats, spent significantly longer time in the target quadrant compared to non-target quadrants suggesting that DFP intoxication caused significant memory deficits (Fig. 3Bii). DPO, however, did not mitigate the memory deficit. Representative probe trial traces at 16d post-DFP are illustrated in Figure 3C.

DPO rescues DFP-induced motor learning deficit

Exposure to OP can result in reduced motor function in both animal models of OP intoxication and OP poisoned humans[47,48]. Therefore, to evaluate motor function impairments due to DFP exposure and mitigation by DPO, we employed the rotarod and horizontal bar test (HBT). In rotarod, all rats displayed significantly longer latency to fall after three trials before exposure to DFP, suggesting improved motor learning in all rats after training (Fig. 4A). At 18d post-DFP, vehicle-treated group had a significantly shorter latency to fall compared to the control group. In contrast, DPO treated rats had a significantly longer latency to fall compared to the vehicle-treated group. Both control and DPO groups showed significantly improved motor learning compared to the vehicle-treated group (Fig. 4A).

In HBT, all rats demonstrated significantly shorter time to reach the goal during the test day compared to the training confirming the normal baseline motor activity in all tested rats before DFP exposure (Fig. 4B). At 23d post-DFP, none of the groups showed any differences in latency to reach the platform between training and test periods (Fig. 4B) suggesting neither DFP nor DPO had any impact on linear motor function.

DPO treatment attenuates activated astrogliosis, but not microgliosis, following DFP intoxication at six weeks post-exposure

DFP exposure in rats chronically activates astrocytes and microglia[14,49,50]. The reactive astrogliosis and microgliosis contribute to the generation of ROS/RNS, proinflammatory cytokines, and epileptogenesis[14,51]. Immunohistochemistry of brain sections for GFAP and IBA1 were performed to determine astrogliosis and microgliosis, respectively. To further identify “reactive-type” astrocytes, we double-labeled GFAP with a complement marker, C3[52]. GFAP was used to mark all astrocytic phenotypes, while C3 was to probe activated astrocytes[51,52]. In the DFP-exposed vehicle-treated group, relative to control, a marked increase of GFAP and C3 co-labeled cells were observed in the CA1, CA3, DG hippocampal regions, and the piriform cortex (Fig. 5B, 5C). Representative images of GFAP and C3 co-labeled cells distribution in the CA1 hippocampus from the control, vehicle, and DPO groups are shown in Figure 5A. Linear mixed-effects analysis showed a significant global increase of GFAP and C3 positive astrocytes in the vehicle group, in contrast to the control, and their reduction in the DPO treated group in all brain regions compared to the vehicle group (Fig. 5B, 5C). In all the quantified brain regions, DFP exposure caused a significant increase in both astrogliosis (GFAP positive cells; Fig. 5Bi, ii) and reactive astrogliosis (GFAP+C3 co-labeled cells; Fig. 5Ci, ii). In the DPO group, significantly fewer GFAP positive cells and C3 co-labeled cells in the CA1 region of the hippocampus and piriform cortex were observed when compared to the vehicle-treated group (Fig. 5Bii, 5Cii). In the

dentate gyrus (DG), DPO treated animals did not have significantly reduced GFAP positive cells but, C3 co-labeled cells were significantly reduced (Fig. 5Cii).

Microgliosis was quantified from the immunostained brain sections with IBA1 and a phagocytic marker, CD68. CD68 is a lysosomal protein reported to be increased in microglia in the epileptic human brains and animal models of epilepsy[53]. We and others have demonstrated a significant increase in the CD68 immunopositive microglia in the rat DFP model[14,49]. Representative immunostained IBA1 and CD68 cells in the DG from the control, vehicle, and DPO groups are shown in Figure 5D. IBA1 positive microglia co-labeled with CD68 were significantly upregulated in CA1, CA3, DG, and piriform cortex (PC) in DFP exposed vehicle-treated group when compared to the control (Fig. 5Ei, ii; 5Fi, ii). Both linear mixed effects and regional comparison between the vehicle and DPO showed a reduction (10-15%) in both IBA1 cells and CD68 co-labeled cells, but the differences were not statistically significant (Fig. 5E, 5F).

DPO protects against DFP-induced neurodegeneration at six weeks post-exposure

Neurodegeneration of pyramidal cells is one of the most common consequences of DFP induced long-term neurotoxicity[14,46,54]. Neuronal loss is also observed as early as 24h post-DFP [4] and persists for up to 12 weeks post-DFP[14,46]. NeuN (a neuronal marker) coupled with FJB (a neurodegenerative marker) was used to determine the extent of neurodegeneration. Representative images of NeuN and FJB co-labeled cells distribution in the piriform cortex from the control, vehicle, and DPO groups are shown in Figure 6A. There was a significant increase of FJB positive neurons in CA1, CA3, DG and PC in the vehicle-treated group compared to the control (Fig. 6Bi, ii). In DPO treated rats, significant suppression of FJB positive neurons was observed in CA1, DG, and PC regions compared to the vehicle group (Fig. 6Bi, ii).

DFP exposure increases ROS and RNS markers at six weeks post-exposure, and DPO reduces GP91^{phox} (a NOX2 subunit) and glutathiolated protein in the hippocampus, and serum nitrite levels

OP intoxication induces excessive formation of ROS and RNS, which are known to exacerbate neurodegeneration and neuroinflammation[20,26]. Western blot on hippocampal lysates determined levels of key ROS/RNS markers. Since superoxide anion is a major byproduct of NADPH oxidase activation, the expression of hippocampal GP91^{phox}, the major subunit of NOX2, was investigated. There was a significant increase in GP91^{phox} protein levels in the vehicle group at 6 weeks post-DFP compared to the control. DPO, in contrast to the vehicle, significantly suppressed GP91^{phox} (Fig. 7A, 7B). DFP-induced glutathiolated protein levels (anti-GSH) was also significantly suppressed by DPO (Fig. 7A, 7B). Moreover, DPO treatment also significantly reduced the DFP-induced serum nitrite levels measured at 6 weeks post-exposure (Fig. 7C). The other ROS/RNS markers such as inducible nitric oxide synthase (iNOS), 3-nitrotyrosine (3-NT), and lipid peroxidation derived 4-hydroxynoneal (4-HNE) levels were also significantly upregulated by DFP exposure. Although DPO partly reduced iNOS and 3-NT levels in the hippocampus when compared to the vehicle, the differences were not statistically significant (Fig. 7B).

DPO reduces DFP-induced key pro-inflammatory cytokines and chemokines at six weeks post-exposure

We have recently demonstrated the upregulation of key pro-inflammatory cytokines and chemokines in the rat DFP model at 6 weeks post-exposure[14]. Other studies have also shown that exposure to DFP increases mRNA as well as protein levels of the inflammatory mediators in the hippocampus[55,56]. We determined the expression profiles of proinflammatory (IL-1α, TNF-α, IL-1β, IL-6, IL-17A, IL-18), anti-inflammatory (IL-4, IL-5, IL-10), pleiotropic cytokines (IL-2, IL-12), and chemotactic chemokines (MCP-1, LIX, Eotaxin, VEGF, EGF, Leptin, Fractalkine, IP-10, RANTES) at 6 weeks post-DFP using multiplex immunoassay of hippocampal lysates. The IL-1α, TNF-α, IL-6, IL-17A were significantly upregulated in the DFP-exposed vehicle-treated group compared to the control (Fig. 8A). DPO treatment significantly mitigated the elevated levels of IL-1α, IL-6, IL-17A, suggesting the anti-inflammatory role of DPO. TNF-α was also reduced in DPO group but not statistically significant when compared to the vehicle group. Interestingly, DPO significantly reduced IL-18 protein levels compared to the control groups (Fig. 8A).

The anti-inflammatory cytokine, IL-10 levels were significantly lower in DFP group compared to the control. Although the levels of IL-10 in DPO group were not different from the control group, there was no statistical difference between the groups. IL-4 also showed a similar trend. The pleiotropic cytokines (IL-2 and IL-12) were significantly higher in the vehicle group compared to the control group. DPO significantly decreased the elevated protein levels of IL-2 but not IL-12 (Fig. 8A). The chemokines Eotaxin, EGF, Leptin, Fractalkine, IP-10, and RANTES were significantly upregulated in the vehicle group compared to the control group. DPO significantly suppressed DFP-induced leptin and IP-10 levels (Fig. 8B).

Discussion

We have recently demonstrated the impact of long-term neurotoxicity induced by DFP and the role of reactive nitrogen species in the rat model of OP toxicity[14]. In this study, we demonstrate the role of NOX2-mediated ROS in DFP-induced epileptiform spiking, neuroinflammation, and neurodegeneration and their impact on cognitive and motor functions. As a proof-of-concept, diapocynin, a NOX2 inhibitor, was used to intervene in DFP-induced changes in the brain.

DFP is chemically similar to OP nerve agents such as soman and sarin by inducing acute clinical signs of OP poisoning[37,57]. The seizure induction and subsequent brain pathology caused by DFP are also similar to nerve agents, OP pesticides, and other chemoconvulsants[58-61]. OPNAs irreversibly inhibit acetylcholinesterase (AChE), which clinically manifests as neurological, respiratory, and cardiac symptoms[62-64]. OPNA are also potent seizurogenic neurotoxins[65]. OPNA exposed subjects could develop epilepsy, cognitive dysfunction, and other neurological disorders if not treated adequately[6,7,66-70].

DFP serves as a surrogate for real OPNA-exposure scenarios to test the acute and chronic effects in animal models. The NIH-NIAID Chemical Countermeasures Research Program developed a protocol for animal screening models using DFP to identify and accelerate

investigational new drugs (IND) development for OP chemical threats that target the central nervous system. We modified the protocol to suit a civilian population scenario of OP exposure. The military personnel are pre-medicated with pyridostigmine (PYR), a reversible AChE inhibitor to protect from NA exposure[63,64,71-73]. However, PYR is a poor blood-brain barrier permeable MCM, does not protect the brain from long-term OP toxicity, and have some adverse effects[64,71-73]. Recent reports from the rat DFP model with PYR pre-treatment, administered 30 mins before DFP exposure, demonstrated no significant effect on either behavioral seizures or mortality conforming its limited efficacy as a MCM[74]. Moreover, it is impractical to pre-medicate the entire world population with PYR. Therefore, a rat model without PYR pre-treatment is appropriate to mimic a real-world scenario of mass OP exposure to civilians to test the long-term neuroprotective effects of INDs. We have recently published a fully characterized rat DFP model, without PYR pre-treatment[14], and a similar approach followed in this study to test the efficacy of a novel NOX2 inhibitor, diapocynin.

The diapocynin (5, 5′-dehydrodiacetovanillone) is a dimer of apocynin, an effective NADPH oxidase-2 (NOX2) inhibitor[75-81]. Apocynin (acetovanillone or 4-hydroxy-3-methoxyacetophenone), a vanilla-flavored herb derivative, is a natural antioxidant[77,79]. NOX-mediated oxidative damage to proteins in the postsynaptic density has been reported after transient cerebral ischemia and reperfusion in the rat model[82]. It has been used as an anti-inflammatory medication for many years in Europe and Asia[76]. Apocynin and diapocynin protective effects are attributed to NADPH oxidase antagonistic properties[75,76]. However, apocynin does not effectively get converted into diapocynin *in vivo*[78,81]. Therefore, diapocynin is chemically synthesized by oxidative coupling of two apocynin monomers[79,80]. It is ten times more potent and selective, and 13 times more lipophilic than apocynin[76,83]. In the mouse model of Parkinson's disease, oral administration of synthetic diapocynin at 300mg/kg significantly suppressed ROS, RNS, reactive gliosis, and cytokines[83,84]. In the present study, we tested the same dose of diapocynin but administered twice daily for the first three days of DFP exposure to investigate its protective effects on initial seizures, epileptiform spikes during the first four weeks, neuroinflammation and neurodegeneration, and cognitive and motor function at six weeks post-exposure. In pilot studies, we had tested the effects of 100, 150, 200, and 300 mg/kg diapocynin, administered 30 mins before DFP exposure, to determine the optimum concentration of the drug based on epileptiform spiking activity. Maximum suppression of epileptiform spikes was observed with 300 mg/kg, the dose used in the present study.

Response to DFP exposure at 4 mg/kg via the subcutaneous route in male rats, without PYR pre-treatment, produced varying degrees of initial seizure (SE) severity as expected based on our recent study[14]. Atropine and oxime were administered immediately (<1 min) after DFP exposure to control peripheral effects of excessive acetylcholine and to reactivate AChE[85-87], which minimized mortality. Diazepam was administered to control behavioral seizures. Despite MCM administration, animals developed epileptiform spiking activity which was significantly reduced in DPO treated animals suggesting the role of ROS in exacerbating DFP-induced hyperactivation of neurons. Previous studies in the rat DFP model (1.25 mg/kg, s.c.) also demonstrated the upregulation of both ROS (F2-isoprostanes and F4-neuroprostanes) and RNS (citrulline) during the first three days of DFP exposure[26].

In another rat DFP study, glutathione levels were significantly suppressed, and 3-NT levels were increased in the brain at 24 and 48h after DFP exposure[25]. Increased ROS/RNS contributes to hyperexcitability of neurons (indicated by increased epileptiform spiking) and the reduction by diapocynin in this study suggests the protective effects of a NOX2 inhibitor following OP exposure.

OP exposure, whether acute or chronic, has been known to cause cognitive and motor impairments[15,47-49]. We and others have shown that DFP exposure causes persistent neuronal loss and neuroinflammation[14,49,54,55] in various brain regions that may play a role in motor and cognitive dysfunction. In the present study, we observed cognitive impairment at ten days post-exposure to DFP when compared to the naïve control, which is similar to the findings in the same model that we had reported previously[14]. Therefore, our DFP model is reliable, and the results are reproducible in the vehicle control animals, although the vehicles used in the previous study (sterile distilled water, i.m.) and the present study (10% ethanol) were different. We had also demonstrated significant neurodegeneration (FJB +NeuN) and reactive gliosis in the hippocampus at seven days post-DFP in the rats derived from the same cohort used for behavioral testing[14]. Interestingly, although diapocynin treatment reduced DFP-induced neurodegeneration and reactive gliosis, it did not mitigate DFP-induced cognitive dysfunction. However, diapocynin did counteract the DFP-induced motor dysfunction measured by rotarod (Fig. 4A). Further brain mapping studies such as ROS biomarkers expression in the cognitive and motor pathways are required to understand the differential effects of diapocynin on motor and cognitive functions.

We have previously demonstrated the impact of DFP-induced SE on gliosis and neurodegeneration at both early (7 days post-DFP) and late exposure (12 weeks post-DFP). In another DFP study, neurodegeneration and gliosis were also demonstrated at seven days and two months post-exposure[15,89,90]. In this study, six weeks post-exposure also confirmed a significant increase in both astrogliosis and microgliosis (Fig. 5). Further, we used C3 and CD68 as a marker for reactive astrocytes and microglia, respectively. In this study, we tested the key complement protein C3, a complement pathway activation marker, to identify activated/reactive astrocytes. The complement pathway is an essential signaling component implicated in brain inflammation in neurodegenerative diseases such as Alzheimer's disease[91]. C3 regulates neuron-astroglial homeostasis, and the release of C3 from astrocytes may activate microglia to initiate further release of proinflammatory cytokines and chemokines from the activated glia. Indeed, the key proinflammatory cytokines such as TNF-α, IL-1α, IL-6, and IL-17A were significantly upregulated in DFP exposed animals (Fig.8A). Interestingly, TNF-α promotes C3 activation and release from astrocytes and promotes neurodegeneration[91]. Therefore, blocking C3 activation either directly or by decreasing their levels in astrocytes, may promote neuroprotective pathways[92,93]. In this study, diapocynin treatment significantly reduced C3 positive astrocytes, neurodegeneration (measured by FJB positive neurons), and key proinflammatory cytokines and chemokines (Fig. 5, 8) suggesting the role of NOX2 mediated brain pathogenesis in the DFP model.

Currently, there are no reports on NOX2 and C3 pathway interaction in the brain exposed to OP nerve agents. The C3-NOX2 mediated bacteriolytic effects in neutrophils have been reported[94]. Since microglia are the resident macrophages in the brain, exposure to

neurotoxins and SE induction compromises the blood-brain-barrier integrity and promotes the infiltration of peripheral monocytes and neutrophils[59,95]. Brain infiltrated monocytes and localized reactive gliosis are known to produce reactive oxygen and nitrogen species, proinflammatory cytokines (neuroinflammation), and neurodegeneration[14,95]. We had demonstrated persistent upregulation of iNOS and 3-NT in glia and neurons, respectively, and serum nitrite levels in DFP exposed animals[14]. In the present study, we also observed a similar increase in RNS markers at six weeks post-exposure. Besides, we found a significant increase in ROS markers such as $GP91^{phox}$ (a membrane-associated subunit of NOX2), glutathionylation, and 4-HNE (Fig.7). We had previously shown that SE-induced changes in the hippocampus increase protein kinase C delta (PKCδ)[44]. PKCδ phosphorylates cytosolic $p47^{phox}$ to form a functional NOX2 complex with $GP91^{phox}$ to generate both ROS and RNS through an iNOS-mediated mechanism. Moreover, glutathiolated proteins, a post-translational modification through thiolation of proteins, were shown to be elevated following oxidative injury[96]. Therefore, increased glutathiolated protein levels are indicative of proteotoxic process that could lead to cell death[96,97]. Hippocampal $GP91^{phox}$ and glutathiolated protein levels, and serum nitrite levels, were significantly reduced by diapocynin (Fig. 7A-C), suggesting the antioxidant properties of diapocynin. Moreover, unlike in the short-term study[98], where oxime was not administered, in this study, we had treated the animals with 2-PAM to reactivate AChE. Thus, the levels of AChE might not be suppressed or changed at six weeks post-DFP, and therefore, the long-term pathologies are more likely driven by the initial DFP-induced SE severity. Nonetheless, further studies will inform whether DFP-induced long-term brain pathology can be attributed to a persistent suppression of AChE alone.

In conclusion, diapocynin, a NOX2 inhibitor, promotes neuroprotective effects by suppressing DFP-induced early events of epileptiform spiking, and the subsequent long-term effects such as persistent reactive astrogliosis, ROS, and proinflammatory cytokines. Although diapocynin decreased reactive microglia, the difference was not statistically significant, which may imply that NOX2 mediated mechanism in the DFP model is largely mediated by astrocytes, perhaps via C3 mediated mechanism, or a different mechanism such as NOX1-dependent NADPH oxidase in microglia[77].

Supplementary Material

Refer to Web version on PubMed Central for supplementary material.

Acknowledgments and authors contribution

This project is funded by National Institutes of Health (NIH), the National Institute of Neurological Disorder and Stroke (NINDS), CounterACT program (1R21 NS099007; PI- T. Thippeswamy). TT conceived the idea, designed the experiments, and led the project. M.P conducted most of the experiments, analyzed the data, and drafted some aspects of the manuscript. M.G., S.S., C.G., G.G., V.A. assisted in some of the experiments, blinding the experiments/samples and data cross verification.

References

1. Wiercinski A & Jackson JP. 2019 Nerve Agents In StatPearls Treasure Island (FL): StatPearls Publishing.

2. Organization W.H. & U.N.E. Programme. 1990 “Public health impact of pesticides used in agriculture.” World Health Organization.

3. OPCW Report. 2017OPCW 6 30, 2017 Accessed November 11, 2018 https://www.opcw.org/media-centre/news/2017/06/opcw-fact-finding-mission-confirms-use-chemical-weapons-khan-shaykhun-4.

4. UN Report. 20139 16, 2013 Accessed November 11, 2018 https://undocs.org/A/67/997.

5. Vale JA, OBE TCM & CBE RLM. 2018 Novichok: a murderous nerve agent attack in the UK. Clin. Toxicol 56: 1093–1097.

6. Suzuki T, Morita H, Ono K, et al. 1995 Sarin poisoning in Tokyo subway. Lancet Lond. Engl 345: 980.

7. Dolgin E 2013 Syrian gas attack reinforces need for better anti-sarin drugs. Nat. Med 19: 1194–1195. [PubMed: 24100968]

8. Zarocostas J 2017 Syria chemical attacks: preparing for the unconscionable. Lancet Lond. Engl 389: 1501.

9. Chen Y 2012 Organophosphate-induced brain damage: Mechanisms, neuropsychiatric and neurological consequences, and potential therapeutic strategies. NeuroToxicology 33: 391–400. [PubMed: 22498093]

10. Henretig FM, Kirk MA & McKay CA. 2019 Hazardous Chemical Emergencies and Poisonings. N. Engl. J. Med 380: 1638–1655. [PubMed: 31018070]

11. Jett DA, Galanopoulou AS & Moshé SL. 2019 Preface: Discovery and development of better medical countermeasures for chemical threats targeting the nervous system. Neurobiol. Dis 104557.

12. National Toxicology Program. 2019 Systematic Review of the Long-term Neurological Effects Following Acute Exposure to Sarin National Toxicology Program, Washington DC. .

13. Rojas A, Ganesh T, Manji Z, et al. 2016 Inhibition of the prostaglandin E2 receptor EP2 prevents status epilepticus-induced deficits in the novel object recognition task in rats. Neuropharmacology 110: 419–430. [PubMed: 27477533]

14. Putra M, Sharma S, Gage M, et al. 2019 Inducible nitric oxide synthase inhibitor, 1400 W, mitigates DFP-induced long-term neurotoxicity in the rat model. Neurobiol. Dis

15. Flannery BM, Bruun DA, Rowland DJ, et al. 2016 Persistent neuroinflammation and cognitive impairment in a rat model of acute diisopropylfluorophosphate intoxication. J. Neuroinflammation 13: 267. [PubMed: 27733171]

16. Reddy DS & Kuruba R. 2013 Experimental Models of Status Epilepticus and Neuronal Injury for Evaluation of Therapeutic Interventions. Int. J. Mol. Sci 14: 18284–18318. [PubMed: 24013377]

17. Collombet J-M 2011 Nerve agent intoxication: Recent neuropathophysiological findings and subsequent impact on medical management prospects. Toxicol. Appl. Pharmacol 255: 229–241. [PubMed: 21791221]

18. Aroniadou-Anderjaska V, Figueiredo TH, Apland JP, et al. 2016 Long-term neuropathological and behavioral impairments after exposure to nerve agents. Ann. N. Y. Acad. Sci 1374: 17–28. [PubMed: 27002925]

19. Jett DA 2007 Neurological aspects of chemical terrorism. Ann. Neurol 61: 9–13. [PubMed: 17262854]

20. Pearson JN & Patel M. 2016 The role of oxidative stress in organophosphate and nerve agent toxicity. Ann. N. Y. Acad. Sci 1378: 17–24. [PubMed: 27371936]

21. Vanova N, Pejchal J, Herman D, et al. 2018 Oxidative stress in organophosphate poisoning: role of standard antidotal therapy. J. Appl. Toxicol 38: 1058–1070. [PubMed: 29516527]

22. Ranjbar A, Solhi H, Mashayekhi FJ, et al. 2005 Oxidative stress in acute human poisoning with organophosphorus insecticides; a case control study. Environ. Toxicol. Pharmacol 20: 88–91. [PubMed: 21783573]

23. Shadnia S, Azizi E, Hosseini R, et al. 2005 Evaluation of oxidative stress and genotoxicity in organophosphorus insecticide formulators. Hum. Exp. Toxicol 24: 439–445. [PubMed: 16235732]

24. Ranjbar A, Pasalar P & Abdollahi M. 2002 Induction of oxidative stress and acetylcholinesterase inhibition in organophosphorous pesticide manufacturing workers. Hum. Exp. Toxicol 21: 179–182. [PubMed: 12099619]

25. Liang L-P, Pearson-Smith JN, Huang J, et al. 2019 Neuroprotective effects of a catalytic antioxidant in a rat nerve agent model. Redox Biol. 20: 275–284. [PubMed: 30384261]
26. Zaja-Milatovic S, Gupta RC, Aschner M, et al. 2009 Protection of DFP-Induced Oxidative Damage and Neurodegeneration by Antioxidants and NMDA Receptor Antagonist. Toxicol. Appl. Pharmacol 240: 124–131. [PubMed: 19615394]
27. Gultekin F, Ozturk M & Akdogan M. 2000 The effect of organophosphate insecticide chlorpyrifos-ethyl on lipid peroxidation and antioxidant enzymes (in vitro). Arch. Toxicol 74: 533–538. [PubMed: 11131033]
28. Ma MW, Wang J, Zhang Q, et al. 2017 NADPH oxidase in brain injury and neurodegenerative disorders. Mol. Neurodegener 12: 7. [PubMed: 28095923]
29. Cooney SJ, Bermudez-Sabogal SL & Byrnes KR. 2013 Cellular and temporal expression of NADPH oxidase (NOX) isotypes after brain injury. J. Neuroinflammation 10: 917.
30. Patel M, Li Q-Y, Chang L-Y, et al. 2005 Activation of NADPH oxidase and extracellular superoxide production in seizure-induced hippocampal damage. J. Neurochem 92: 123–131. [PubMed: 15606902]
31. Puttachary S, Sharma S, Stark S, et al. 2015. Seizure-Induced Oxidative Stress in Temporal Lobe Epilepsy. BioMed Res. Int 2015:.
32. Kim JH, Jang BG, Choi BY, et al. 2013 Post-treatment of an NADPH oxidase inhibitor prevents seizure-induced neuronal death. Brain Res. 1499: 163–172. [PubMed: 23313582]
33. Shekh-Ahmad T, Lieb A, Kovac S, et al. 2019 Combination antioxidant therapy prevents epileptogenesis and modifies chronic epilepsy. Redox Biol. 26: 101278. [PubMed: 31382215]
34. Lee SH, Choi BY, Kho AR, et al. 2018 Inhibition of NADPH Oxidase Activation by Apocynin Rescues Seizure-Induced Reduction of Adult Hippocampal Neurogenesis. Int. J. Mol. Sci 19: 3087.
35. Puttachary S, Sharma S, Thippeswamy A, et al. 2016 Immediate epileptogenesis: Impact on brain in C57BL/6J mouse kainate model. Front. Biosci. Elite Ed 8: 390–411. [PubMed: 27100347]
36. El Sayed S, Pascual L, Agostini A, et al. 2014 A Chromogenic Probe for the Selective Recognition of Sarin and Soman Mimic DFP. ChemistryOpen 3: 142–145. [PubMed: 25478309]
37. McCarren HS & McDonough JH. 2016 Anticonvulsant discovery through animal models of status epilepticus induced by organophosphorus nerve agents and pesticides. Ann. N. Y. Acad. Sci 1374: 144–150. [PubMed: 27258770]
38. Tripathi HL & Dewey WL. 1989 Comparison of the effects of diisopropylfluorophosphate, sarin, soman, and tabun on toxicity and brain acetylcholinesterase activity in mice. J. Toxicol. Environ. Health 26: 437–446. [PubMed: 2709438]
39. Kilkenny C, Browne WJ, Cuthill IC, et al. 2010 Improving Bioscience Research Reporting: The ARRIVE Guidelines for Reporting Animal Research. PLoS Biol. 8:.
40. Kim Y-B, Hur G-H, Shin S, et al. 1999 Organophosphate-induced brain injuries: delayed apoptosis mediated by nitric oxide. Environ. Toxicol. Pharmacol 7: 147–152. [PubMed: 21781920]
41. Williams PA, White AM, Clark S, et al. 2009 Development of Spontaneous Recurrent Seizures after Kainate-Induced Status Epilepticus. J. Neurosci 29: 2103–2112. [PubMed: 19228963]
42. Vorhees CV & Williams MT. 2006 Morris water maze: procedures for assessing spatial and related forms of learning and memory. Nat. Protoc 1: 848–858. [PubMed: 17406317]
43. Beamer E, Otahal J, Sills GJ, et al. 2012 N w-Propyl-l-arginine (L-NPA) reduces status epilepticus and early epileptogenic events in a mouse model of epilepsy: behavioural, EEG and immunohistochemical analyses. Eur. J. Neurosci 36: 3194–3203. [PubMed: 22943535]
44. Sharma S, Carlson S, Puttachary S, et al. 2018 Role of the Fyn-PKCδ signaling in SE-induced neuroinflammation and epileptogenesis in experimental models of temporal lobe epilepsy. Neurobiol. Dis 110: 102–121. [PubMed: 29197620]
45. Sharma S, Puttachary S, Thippeswamy A, et al. 2018 Status Epilepticus: Behavioral and Electroencephalography Seizure Correlates in Kainate Experimental Models. Front. Neurol 9:.
46. Rojas A, Ganesh T, Lelutiu N, et al. 2015 Inhibition of the prostaglandin EP2 receptor is neuroprotective and accelerates functional recovery in a rat model of organophosphorus induced status epilepticus. Neuropharmacology 93: 15–27. [PubMed: 25656476]

47. Proctor SP, Heaton KJ, Heeren T, et al. 2006 Effects of sarin and cyclosarin exposure during the 1991 Gulf War on neurobehavioral functioning in US army veterans. NeuroToxicology 27: 931–939. [PubMed: 16982099]
48. Landauer MR & Romano JA. 1984 Acute behavioral toxicity of the organophosphate sarin in rats. Neurobehav. Toxicol. Teratol 6: 239–243. [PubMed: 6493427]
49. Guignet M, Dhakal K, Flannery BM, et al. 2019 Persistent behavior deficits, neuroinflammation, and oxidative stress in a rat model of acute organophosphate intoxication. Neurobiol. Dis
50. Liu W, Tang Y & Feng J. 2011 Cross talk between activation of microglia and astrocytes in pathological conditions in the central nervous system. Life Sci. 89: 141–146. [PubMed: 21684291]
51. Zhao X, Liao Y, Morgan S, et al. 2018 Noninflammatory Changes of Microglia Are Sufficient to Cause Epilepsy. Cell Rep. 22: 2080–2093. [PubMed: 29466735]
52. Liddelow SA, Guttenplan KA, Clarke LE, et al. 2017 Neurotoxic reactive astrocytes are induced by activated microglia. Nature 541: 481–487. [PubMed: 28099414]
53. Boer K, Spliet WGM, van Rijen PC, et al. 2006 Evidence of activated microglia in focal cortical dysplasia. J. Neuroimmunol 173: 188–195. [PubMed: 16483671]
54. Kadriu B, Gocel J, Larson J, et al. 2011 Absence of tolerance to the anticonvulsant and neuroprotective effects of imidazenil against DFP-induced seizure and neuronal damage. Neuropharmacology 61: 1463–1469. [PubMed: 21903116]
55. Rojas A, Wang W, Glover A, et al. 2018 Beneficial Outcome of Urethane Treatment Following Status Epilepticus in a Rat Organophosphorus Toxicity Model. eNeuro 5: ENEURO.0070–18.2018.
56. Hobson BA, Sisó S, Rowland DJ, et al. 2017 From the Cover: Magnetic Resonance Imaging Reveals Progressive Brain Injury in Rats Acutely Intoxicated With Diisopropylfluorophosphate. Toxicol. Sci 157: 342–353. [PubMed: 28329842]
57. Lynch MR, Andrea Rice M & Robinson SE. 1986 Dissociation of locomotor depression and ChE activity after DFP, soman and sarin. Pharmacol. Biochem. Behav 24: 941–947. [PubMed: 3714785]
58. de Araujo Furtado M, Lumley LA, Robison C, et al. 2010 Spontaneous recurrent seizures after status epilepticus induced by soman in Sprague-Dawley rats. Epilepsia 51: 1503–1510. [PubMed: 20067510]
59. Puttachary S, Sharma S, Verma S, et al. 2016 1400W, a highly selective inducible nitric oxide synthase inhibitor is a potential disease modifier in the rat kainate model of temporal lobe epilepsy. Neurobiol. Dis 93: 184–200. [PubMed: 27208748]
60. Todorovic MS, Cowan ML, Balint CA, et al. 2012 Characterization of status epilepticus induced by two organophosphates in rats. Epilepsy Res. 101: 268–276. [PubMed: 22578704]
61. Deshpande LS, Carter DS, Blair RE, et al. 2010 Development of a Prolonged Calcium Plateau in Hippocampal Neurons in Rats Surviving Status Epilepticus Induced by the Organophosphate Diisopropylfluorophosphate. Toxicol. Sci 116: 623–631. [PubMed: 20498005]
62. Auta J, Costa E, Davis J, et al. 2004 Imidazenil: a potent and safe protective agent against diisopropyl fluorophosphate toxicity. Neuropharmacology 46: 397–403. [PubMed: 14975695]
63. Miller SA, Blick DW, Kerenyi SZ, et al. 1993 Efficacy of physostigmine as a pretreatment for organophosphate poisoning. Pharmacol. Biochem. Behav 44: 343–347. [PubMed: 8446666]
64. Kerenyi SZ, Murphy MR & Hartgraves SL. 1990 Toxic interactions between repeated soman and chronic pyridostigmine in rodents. Pharmacol. Biochem. Behav 37: 267–271. [PubMed: 2080189]
65. Jett DA 2012 Chemical toxins that cause seizures. Neurotoxicology 33: 1473–1475. [PubMed: 23085523]
66. Miyaki K, Nishiwaki Y, Maekawa K, et al. 2005 Effects of sarin on the nervous system of subway workers seven years after the Tokyo subway sarin attack. J. Occup. Health 47: 299–304. [PubMed: 16096354]
67. Morita H, Yanagisawa N, Nakajima T, et al. 1995 Sarin poisoning in Matsumoto, Japan. Lancet Lond. Engl 346: 290–293.
68. Yanagisawa N, Morita H & Nakajima T. 2006 Sarin experiences in Japan: acute toxicity and long-term effects. J. Neurol. Sci 249: 76–85. [PubMed: 16962140]

69. Murata K, Araki S, Yokoyama K, et al. 1997 Asymptomatic sequelae to acute sarin poisoning in the central and autonomic nervous system 6 months after the Tokyo subway attack. J. Neurol 244: 601–606. [PubMed: 9402534]
70. Fields RD 2017Scientific American Blog Network 4 12, 2017 Accessed November 13, 2018 https://blogs.scientificamerican.com/guest-blog/survivors-of-the-gas-attack-in-syria-face-long-term-illness/.
71. Grunwald J, Raveh L, Doctor BP, et al. 1994 Huperzine A as a pretreatment candidate drug against nerve agent toxicity. Life Sci. 54: 991–997. [PubMed: 8139389]
72. Coelho F & Birks J. 2001 Physostigmine for Alzheimer's disease. Cochrane Database Syst. Rev CD001499.
73. Philippens IH, Wolthuis OL, Busker RW, et al. 1996 Side effects of physostigmine as a pretreatment in guinea pigs. Pharmacol. Biochem. Behav 55: 99–105. [PubMed: 8870044]
74. Bruun DA, Guignet M, Harvey DJ, et al. 2019 Pretreatment with pyridostigmine bromide has no effect on seizure behavior or 24 hour survival in the rat model of acute diisopropylfluorophosphate intoxication. NeuroToxicology 73: 81–84. [PubMed: 30853371]
75. Kanegae MPP, Condino-Neto A, Pedroza LA, et al. 2010 Diapocynin versus apocynin as pretranscriptional inhibitors of NADPH oxidase and cytokine production by peripheral blood mononuclear cells. Biochem. Biophys. Res. Commun 393: 551–554. [PubMed: 20171179]
76. Palmen MJHJ, Beukelman CJ, Mooij RGM, et al. 1995 Anti-inflammatory effect of apocynin, a plant-derived NADPH oxidase antagonist, in acute experimental colitis. Neth. J. Med 2: A41.
77. Chéret C, Gervais A, Lelli A, et al. 2008 Neurotoxic activation of microglia is promoted by a nox1-dependent NADPH oxidase. J. Neurosci. Off. J. Soc. Neurosci 28: 12039–12051.
78. Ismail HM, Scapozza L, Ruegg UT, et al. 2014 Diapocynin, a Dimer of the NADPH Oxidase Inhibitor Apocynin, Reduces ROS Production and Prevents Force Loss in Eccentrically Contracting Dystrophic Muscle. PLoS ONE 9:.
79. Luchtefeld R, Luo R, Stine K, et al. 2008 Dose formulation and analysis of diapocynin. J. Agric. Food Chem 56: 301–306. [PubMed: 18092754]
80. Luchtefeld R, Dasari MS, Richards KM, et al. 2008 Synthesis of Diapocynin. J. Chem. Educ 85: 411.
81. Wang Q, Smith RE, Luchtefeld R, et al. 2008 Bioavailability of apocynin through its conversion to glycoconjugate but not to diapocynin. Phytomedicine Int. J. Phytother. Phytopharm 15: 496–503.
82. Murotomi K, Takagi N, Takeo S, et al. 2011 NADPH oxidase-mediated oxidative damage to proteins in the postsynaptic density after transient cerebral ischemia and reperfusion. Mol. Cell. Neurosci 46: 681–688. [PubMed: 21262362]
83. Ghosh A, Kanthasamy A, Joseph J, et al. 2012 Anti-inflammatory and neuroprotective effects of an orally active apocynin derivative in pre-clinical models of Parkinson's disease. J. Neuroinflammation 9: 241. [PubMed: 23092448]
84. Dranka BP, Gifford A, Ghosh A, et al. 2013 Diapocynin prevents early Parkinson's disease symptoms in the Leucine-Rich Repeat Kinase 2 (LRRK2R1441G) transgenic mouse. Neurosci. Lett 549: 57–62. [PubMed: 23721786]
85. Wright LKM, Liu J, Nallapaneni A, et al. 2010 Behavioral sequelae following acute diisopropylfluorophosphate intoxication in rats: comparative effects of atropine and cannabinomimetics. Neurotoxicol. Teratol 32: 329–335. [PubMed: 20034559]
86. Pibiri F, Kozikowski AP, Pinna G, et al. 2008 The combination of huperzine A and imidazenil is an effective strategy to prevent diisopropyl fluorophosphate toxicity in mice. Proc. Natl. Acad. Sci. U. S. A 105: 14169–14174. [PubMed: 18784370]
87. Shih T-M, Rowland TC & McDonough JH. 2007 Anticonvulsants for nerve agent-induced seizures: The influence of the therapeutic dose of atropine. J. Pharmacol. Exp. Ther 320: 154–161. [PubMed: 17015638]
88. Hånell A & Marklund N. 2014 Structured evaluation of rodent behavioral tests used in drug discovery research. Front. Behav. Neurosci 8:.
89. Sisó S, Hobson BA, Harvey DJ, et al. 2017 Editor's Highlight: Spatiotemporal Progression and Remission of Lesions in the Rat Brain Following Acute Intoxication With Diisopropylfluorophosphate. Toxicol. Sci 157: 330–341. [PubMed: 28329845]

90. Liu C, Li Y, Lein PJ, et al. 2012 Spatiotemporal patterns of GFAP upregulation in rat brain following acute intoxication with diisopropylfluorophosphate (DFP). Curr. Neurobiol 3: 90–97. [PubMed: 24039349]

91. Lian H, Yang L, Cole A, et al. 2015 NFκB-Activated Astroglial Release of Complement C3 Compromises Neuronal Morphology and Function Associated with Alzheimer's Disease. Neuron 85: 101–115. [PubMed: 25533482]

92. Fonseca MI, Ager RR, Chu S-H, et al. 2009 Treatment with a C5aR antagonist decreases pathology and enhances behavioral performance in murine models of Alzheimer's disease. J. Immunol. Baltim. Md 1950 183: 1375–1383.

93. Leinhase I, Schmidt OI, Thurman JM, et al. 2006 Pharmacological complement inhibition at the C3 convertase level promotes neuronal survival, neuroprotective intracerebral gene expression, and neurological outcome after traumatic brain injury. Exp. Neurol 199: 454–464. [PubMed: 16545803]

94. Woodman ME, Worth RG & Wooten RM. 2012 Capsule influences the deposition of critical complement C3 levels required for the killing of Burkholderia pseudomallei via NADPH-oxidase induction by human neutrophils. PloS One 7: e52276. [PubMed: 23251706]

95. Varvel NH, Neher JJ, Bosch A, et al. 2016 Infiltrating monocytes promote brain inflammation and exacerbate neuronal damage after status epilepticus. Proc. Natl. Acad. Sci 113: E5665–E5674. [PubMed: 27601660]

96. Hill BG, Ramana KV, Cai J, et al. 2010 Measurement and identification of S-glutathiolated proteins. Methods Enzymol. 473: 179–197. [PubMed: 20513478]

97. Cholanians AB, Phan AV, Ditzel EJ, et al. 2016 From the Cover: Arsenic Induces Accumulation of α-Synuclein: Implications for Synucleinopathies and Neurodegeneration. Toxicol. Sci 153: 271–281. [PubMed: 27413109]

98. Rojas A, Ganesh T, Wang W, et al. 2019 A rat model of organophosphate-induced status epilepticus and the beneficial effects of EP2 receptor inhibition. Neurobiol. Dis

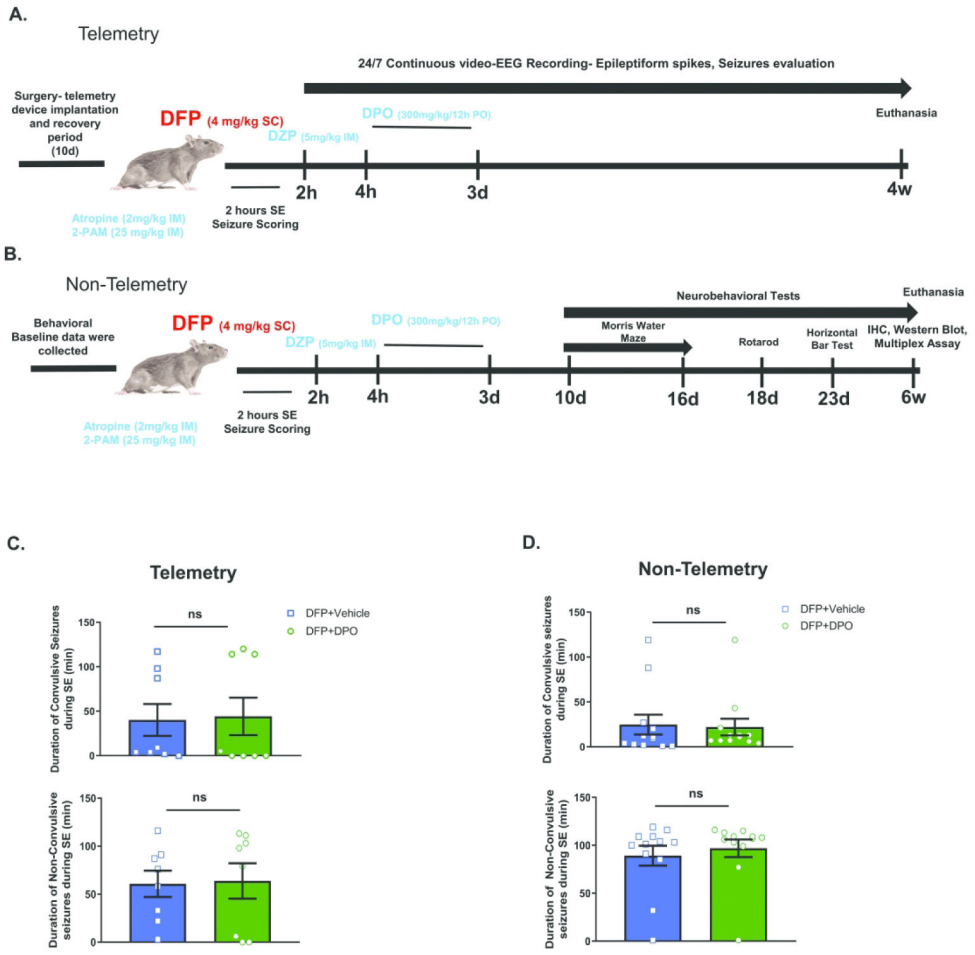

Figure 1.

Experimental designs. A) EEG electrodes were implanted 10d before DFP administration. Two hours after DFP, diazepam was administered and a further 2h later DPO or vehicle was administered twice daily for three days. Video-EEG recorded for four weeks. B) Non-telemetered animals were used for behavioral data which was collected before and after the DFP exposure. DPO treatment was similar to the telemetry group. Animals were euthanized and brains processed for immunohistochemistry, Western blot, and multiplex assays. C, D) Initial SE severity quantification following acute DFP intoxication in telemetry animals and non-telemetry animals. In both groups, SE severity was scored in real-time and verified with video recordings. Data presented as mean ± SEM. There were no significant differences in the SE severity (convulsive or non-convulsive) between the vehicle and DPO treated groups in both telemetry and non-telemetry groups. (n=8 in telemetry group, n=12 in non-telemetry group, ns=non-significant).

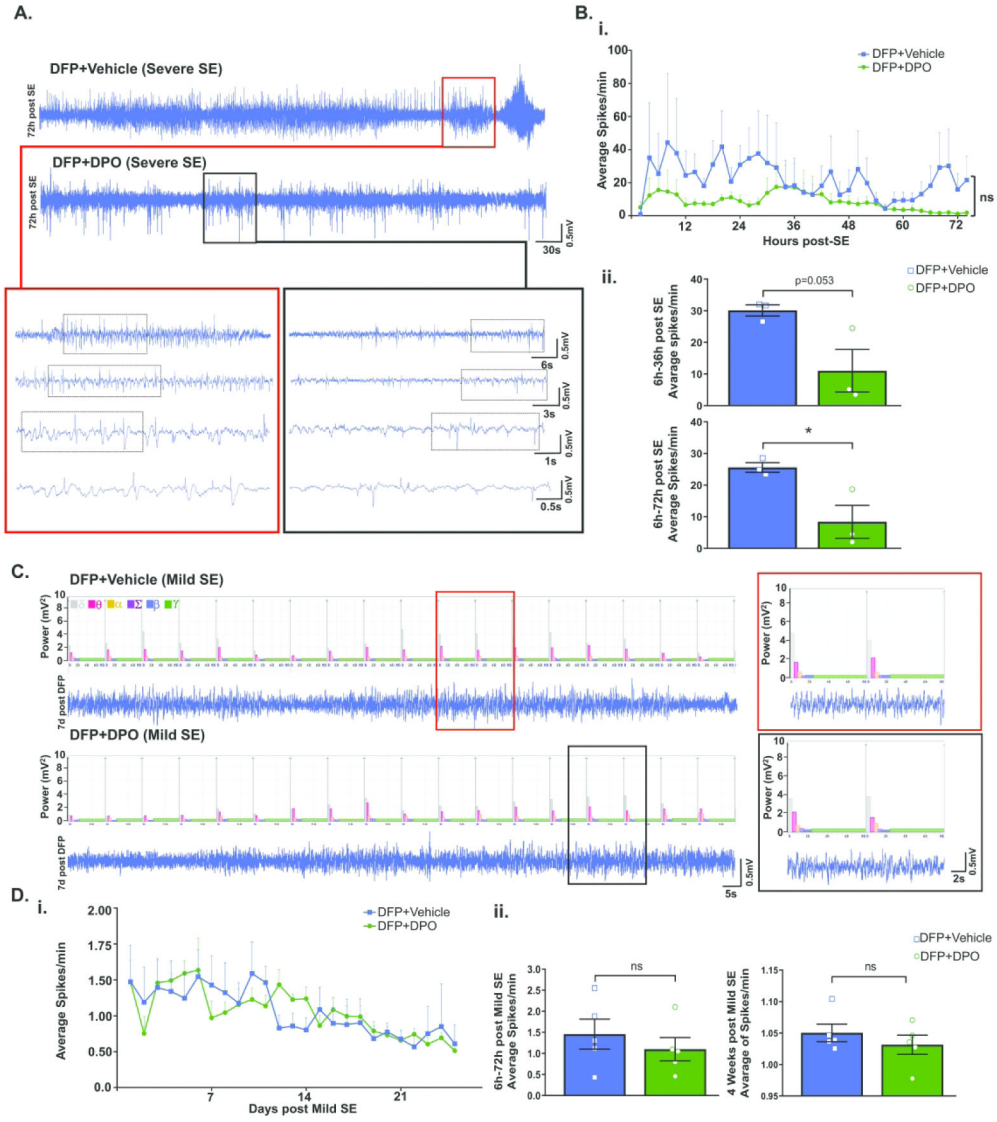

Figure 2.

EEG characteristics of DFP-induced seizures. A) Representative EEG traces of severe SE rats at 72h following DFP in vehicle and DPO groups. Bi) A comparison of the average of spikes per min from both groups within 72h of treatment period. (Bii) Cumulative data comparison of both vehicle and DPO groups between 6h and 36h and 6h and 72h. DPO significantly suppressed spike rate during the first 6-72h post-exposure. C) Representative EEG traces of rats with mild to moderate SE 7 days following DFP. Di) Spike rate comparison between vehicle and DPO groups throughout the four weeks in mild to moderate SE rats. Dii) Pooled data comparison of average spikes between 6h and 72h and full course of four weeks in the mild to moderate SE rats. Data presented as mean ± SEM (n=3 in Severe SE, n=5 in mild to moderate SE, ns=non-significant, *p<0.05).

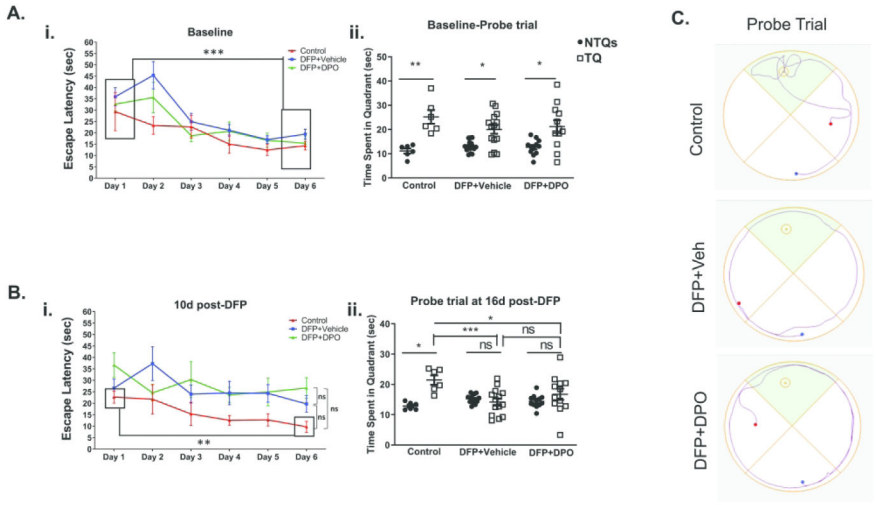

Figure 3.

Impact of DFP exposure and DPO treatment in cognition, the Morris Water Maze test. Ai, ii) Before DFP exposure (baseline), the learning curves were normal and no differences in the time spent in quadrants for all groups. Bi) Escape latencies at 10d post-DFP showed no differences between groups. Bii) DFP treated animals did not spend significantly more time in the target quadrant than non-target quadrants whereas control stayed significantly longer. There was a significant reduction of time spent in the target quadrant in both vehicle and DPO groups when compared to the control group. C) Representative probe trial traces at 16d post-DFP. Data presented as mean ± SEM (n=6-14, ns=non-significant, *p<0.05, **p<0.01, ***p<0.001).

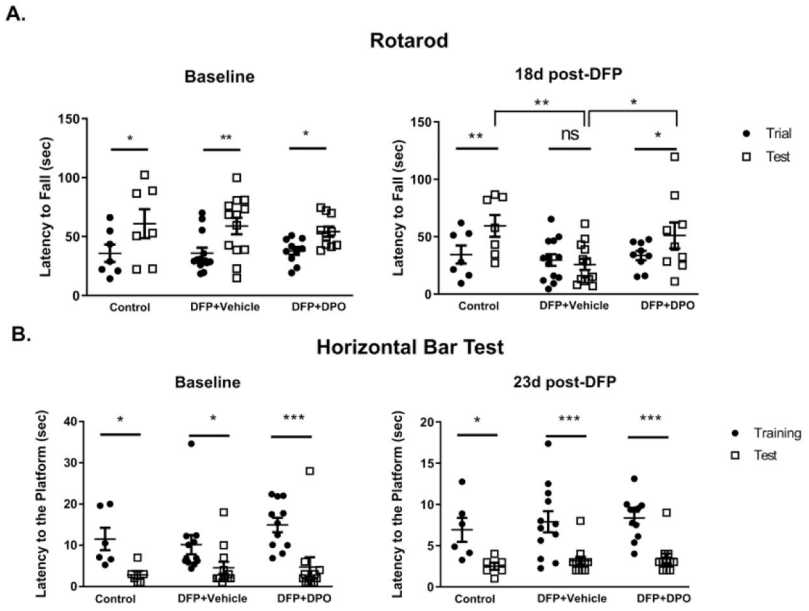

Figure 4.

DPO treatment mitigated DFP-induced motor dysfunction. A-B) During pre-DFP exposure period (baseline), there were significant differences between the training and test periods in all three groups, in both Rotarod and Horizontal bar tests, suggesting the animals had normal motor function. A) Baseline vs. post-DFP performances on Rotarod test. At 18d post-DFP, DPO-treated and the (naïve) control groups showed significantly longer latency to fall during the test period on the rotarod test when compared to the vehicle-treated DFP exposed group. B) All groups significantly improved their performance on the Horizontal Bar test at 23d post-DFP regardless of the treatments. Data presented as mean ± SEM (n=6-14, ns=non-significant, *p<0.05, **p<0.01, ***p<0.001).

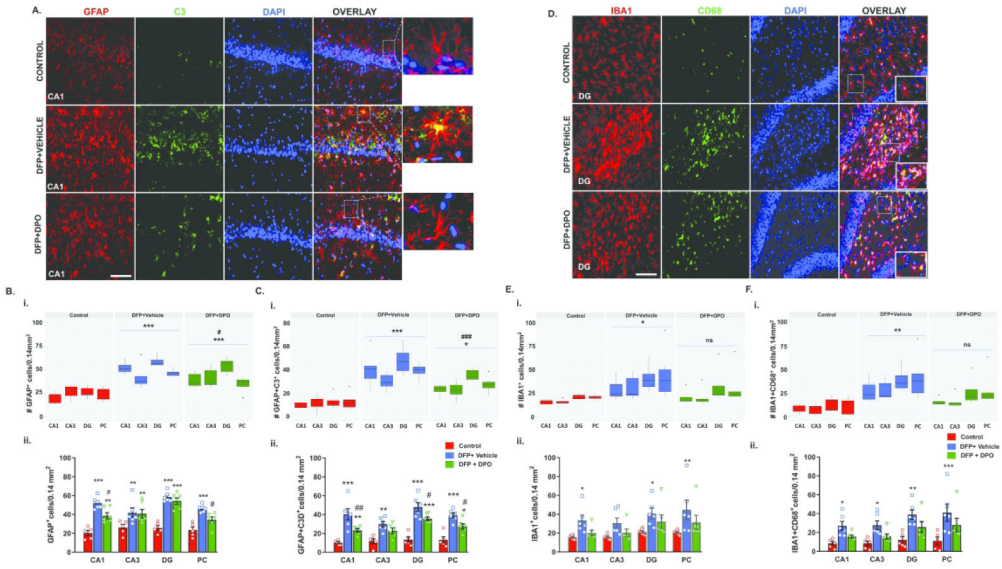

Figure 5.

DPO attenuated DFP-induced activated astrogliosis, but not microgliosis, at six weeks post-DFP. A-C) Representative images of brain sections (CA1 hippocampus) immunostained for GFAP (astrocytic marker, red) and C3 (a marker for activated astrocytes, green), and the cell quantification from the hippocampus and piriform cortex (PC) (Bi, ii, Ci, ii; linear mixed-effect model and region-wise analysis). DPO significantly reduced DFP-induced reactive astrogliosis. Scale bar 100μm. D) Representative images of brain sections (CA1 hippocampus) immunostained for IBA1 (microglia marker, red) and CD68 (phagocytic marker, green), and the cell quantification (E, F). Both mixed-effects model and region-wise analysis showed significant upregulation of phagocytic microglia in the hippocampus and PC (Ei, ii; Fi, ii). DPO appeared to show a degree of reduced microgliosis but this was statistically insignificant. Scale bar 100μm. Data presented as mean ± SEM for region wise comparison (ii) and as a group median (i) and 95% CI (n=6-7, *p<0.05, **p<0.01, ***p<0.001 vs. control; ns=non-significant, #p<0.05, ##p<0.01, ###p<0.001 vs. DFP +vehicle).

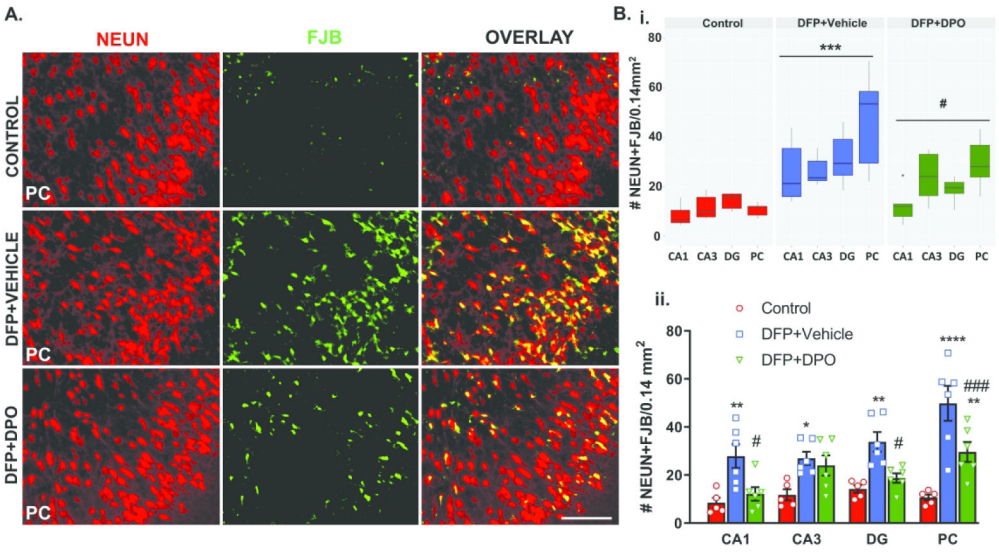

Figure 6.

DPO prevented DFP-induced neurodegeneration at six weeks post-exposure. A) Double immunostaining of brain sections for a neuronal marker, NeuN (red), and FlouroJade B (FJB, green), a marker for dying neurons. A mixed-effect analysis for neurodegeneration in overall analyzed brain regions revealed a significant increase of FJB positive neurons in the vehicle-treated group as compared to the controls. DPO treatment significantly mitigated the DFP-induced neurodegeneration (Bi). Region-specific comparisons between groups are reported in the panel (Bii). Scale bar 100 μm. Data presented as mean ± SEM for region wise comparison (ii) and as a group median (i) and 95% CI (n=5-6, *p<0.05, **p<0.01, ***p<0.001, ****p<0.0001 vs. control; ns=non-significant, #p<0.05, ###p<0.001 vs. DFP +vehicle).

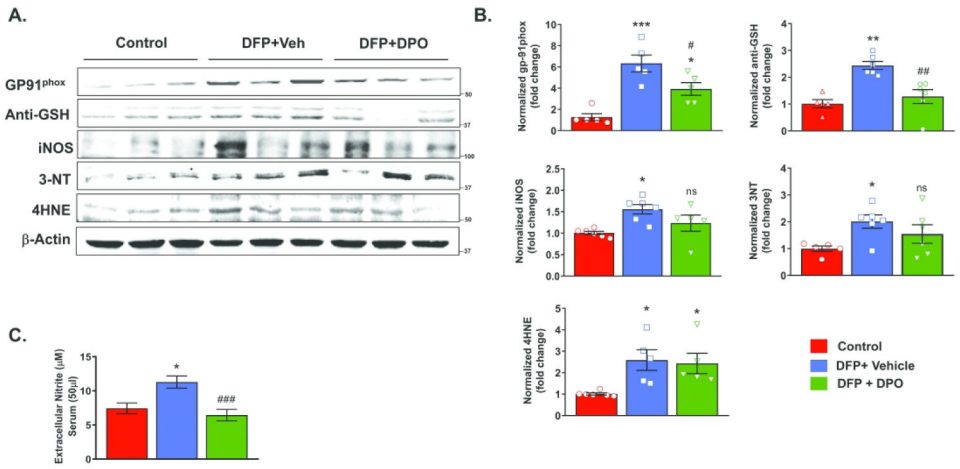

Figure 7.

DFP exposure caused a persistent elevation of ROS and RNS markers at six weeks post-exposure. Representative Western blots of GP91phox, (anti-GSH) glutathiolated protein, iNOS, 3NT, 4-HNE from control, vehicle, and DPO treated groups. B) DFP exposure significantly increased the levels of GP91phox, glutathiolated protein, iNOS, 3NT, 4-HNE when compared to the control. DPO treatment significantly reduced DFP-induced GP91phox and glutathiolated protein levels, but not iNOS, 3NT, and 4-HNE. C) DPO significantly reduced DFP-induced increased extracellular serum nitrite. Data presented as mean ± SEM (n=5-6, *p<0.05, **p<0.01, ***p<0.001 vs. control; ns=non-significant, #p<0.05, ##p<0.01, ###p<0.001 vs. DFP+vehicle).

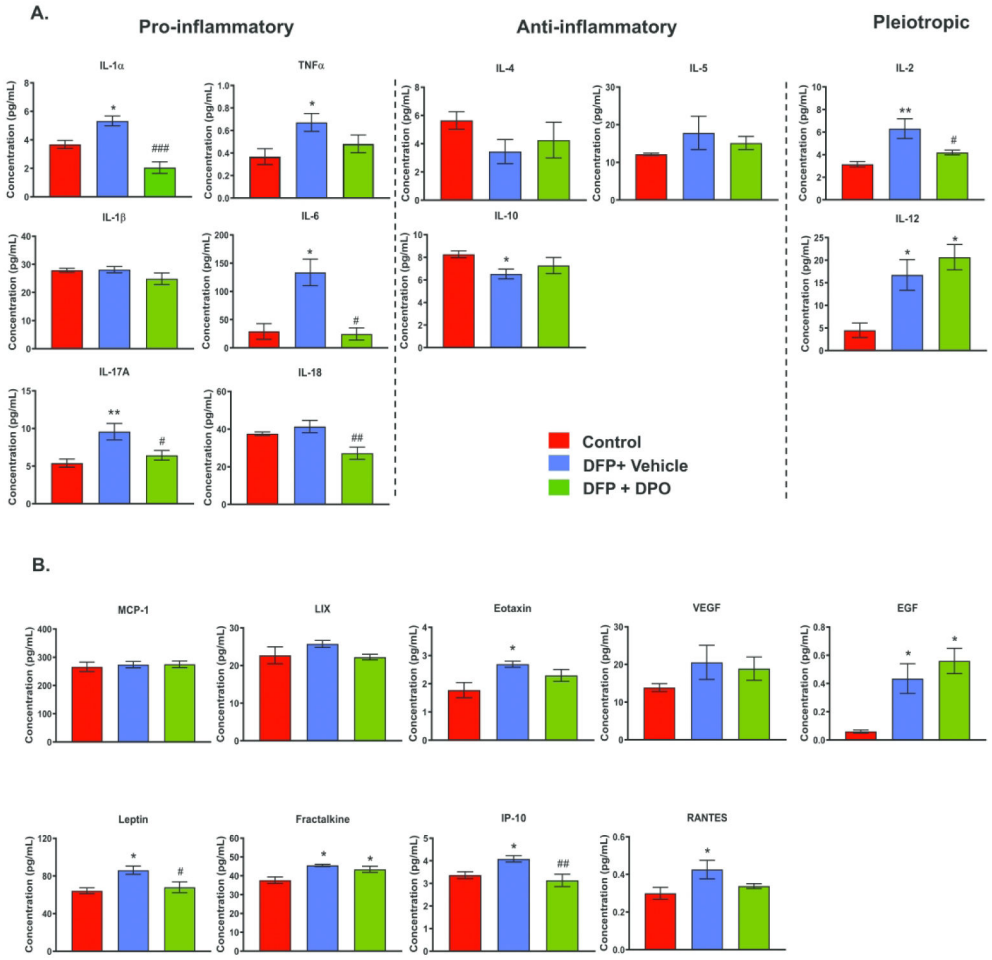

Figure 8.

DPO significantly reduced key proinflammatory cytokines and chemokines in the hippocampus at six weeks post-DFP. A) DFP exposure upregulated IL-1α, TNF-α, IL-6, IL-17A while DPO significantly suppressed IL-6, IL-17A and IL-1α. Exposure to DFP significantly reduced the anti-inflammatory cytokine IL-10 level but DPO had no effect. The pleiotropic cytokines, IL-2 and IL-12, were upregulated in the vehicle group. DPO treatment significantly reduced IL-2 level but did not reduce the DFP-induced levels of IL-12. B) DFP exposure significantly elevated the levels of chemokines and growth factors such as Leptin, Eotaxin, EGF, Fractalkine, IP-10, RANTES. DPO only mitigated the increased levels of leptin and IP-10. Data presented as mean ± SEM (n=4-6, *p<0.05, **p<0.01 vs. control; #p<0.05, ##p<0.01, ###p<0.001 vs. DFP+vehicle).